ELSEVIER

CrossMark

Available online at www.sciencedirect.com

ScienceDirect

Procedia Engineering 81 (2014) 456 – 461

Procedia Engineering

www.elsevier.com/locate/procedia

11th International Conference on Technology of Plasticity, ICTP 2014, 19-24 October 2014, Nagoya Congress Center, Nagoya, Japan

Hot deformation behavior of Fe-Mn-Al light-weight steel

Fu-qiang Yang, Ren-bo Song*, Lei-feng Zhang, Chao Zhao

School of Materials Science and Technology, University of Science and Technology Beijing, No.30, Xueyuan Road, Haidian District, Beijing, 100083, China

Abstract

The hot deformation behaviors Fe-Mn-Al light-weight steel were investigated by means of isothermal compression test within the range of 900~1150 °C at different strain rate of 0.01, 0.1, 1, 1 0 s^{-1} and the maximum deformation degree 60%. The results show that temperature plays an important role in the hot compression deformation of Fe-Mn-Al steel. With the increase of deformation temperature and rate, the recrystallization degree increases gradually and fine austenite structure was obtained and deformed ferrite was kept and distributed perpendicular to compression direction. Based on the stress-strain curves, the activation energy for deformation and thermal deformation equation were derived after fitting analysis of experimental data of dynamic recrystallization. Calculated thermal activation energy was 294.204 kJ/mol with the temperature range of 900~1150 °C. Dynamic recrystallization of experimental steel is sensitive to deformation temperature and strain rate, and increasing deformation temperature or decreasing strain rate would promote dynamic recrystallization and growth for both austenite and ferrite.

Selection and peer-review under responsibility of the Department of Materials Science and Engineering, Nagoya University

Keywords: Fe-Mn-Al steel; Hot compression deformation; Dynamic recrystallization

1. Introduction

Recently Fe-Mn-Al steel has attracted lots of attention for its excellent mechanical properties and lower density, which could be applied in automobile industry to reduce the energy consumption and CO_2 emissions. Addition of high content Mn, Al and C elements makes the steel with high strength (~900MPa) and total elongation (>50%)

* Corresponding author. Tel.: +86-10-82377990.; fax.: +86-10-62334191
E-mail address: songrb@mater.ustb.edu.cn

Selection and peer-review under responsibility of the Department of Materials Science and Engineering, Nagoya University
doi:10.1016/j.proeng.2014.10.022

(Frommeyer et al., 2006). This kind of steel could be distinguished into singe austenite (Yoo and Park, 2008), austenite-based and ferrite-based structures (Suh and Kim, 2013) by the detailed chemical composition. Lots of work has been done on the deformation behaviour and microstructure evolution at room temperature (Jiménez et al., 2010). But the research on hot deformation and dynamic recrystallization is still in blank, especially for the duplex Fe-Mn-Al steel. Dynamic recrystallization is an important mechanism for microstructure control on the grain size and mechanical properties during hot deformation, so the study on the deformation mechanism is very essential. It is known that the coexistence of softer austenite and harder ferrite in the microstructure of duplex steel make the hot deformation complex, but similar to duplex stainless steel studied by Yang at al. (2013) and Balancin et al.(2000). Due to higher stacking fault energy, ferrite undergoes dynamic recovery at the beginning stage of deformation (Momeni and Dehgani, 2011), whereas austenite undergoes only limited dynamic recovery. As the dislocation density increased to a critical value, dynamic recrystallization comes into operation (Duprez et al. 2002). In order to simulate the deformation rule of Fe-Mn-Al steel under hot working condition, the material undergoes extensive plastic deformation under different temperature and strain rate. And the findings can serve as reference for further research.

Nomenclature

σ	Flow stress of hot compression (MPa)
ε	True strain
σ_P	Peak flow stress of hot compression curve (MPa)
T	Absolute temperature (K)
$\dot{\varepsilon}$	Strain rate (s^{-1})
Q	Activation energy (KJ/mol)
R	Molar gas constant (8.314J/(mol*K))
$A(A_1, A_2)$, α, β, $n(n_1)$	Material constants

2. Experiments

A 20 kg ingot of Fe-Mn-Al steel was prepared in vacuum induction melting furnaces with the measured composition of 0.95%C, 0.59%Si, 27.02%Mn, 11.5%Al, 0.043%Nb and Fe in balance (wt, %). Homogenized at 1150 °C for 2 h, the ingot was forged into steel strip with section dimension of 40×80 mm. Samples of Φ8×15 mm were cut off from the strip and turning machined on the surface. Gleeble-1500 thermal simulated test machine was used for compression experiments within the range of 900~1150°C at an interval of 50 °C and at different strain rate of 0.01, 0.1, 1, 10 $s^{-1,}$ respectively. The samples were heated to 1200°C with a constant speed of 10 °C/s and soaked for 12 0 s, then compressed at deformation temperature and water quenched. The compression was carried out to the total true strain of 0.9. Deformed specimens for optical microscopy were sectioned at mid plane perpendicular to the compression axis, then mechanically polished and etched with 4% Nital via ZEISS Image M2m optical microscopy. The measured density by Sartoius BSA 2245 electronic analytical balance is 6.55 g/cm^3, a reduction of 16.6% compared to pure iron.

3. Results and discussion

3.1. Flow stress and true strain

Fig. 1 shows the stress-strain curves of experimental steel deformed at different temperature and strain rate. From the experimental curves, it could be found that the peak flow stress decreases with the increase of temperature and decrease of strain rate, and the value of peak stress at 10 s^{-1} and 900 °C are apparently higher than others. The experimental steel exhibits dynamic recrystallization behaviour under any chosen experimental condition. The flow stress increases to the peak with increasing deformation strain and decreases gradually. At the beginning of deformation, the work hardening effect exceeds that of dynamic softening, resulting into a rapid increase of flow stress. With increasing deformation strain, dynamic recovery and recrystallization begin to work and make the stress increase slowly. As softening mechanism dominates during deformation, the flow stress starts to decrease slowly (Wei et al., 2013). From Fig. 1.b, it is also seen that flow stress for experimental steels dropes slightly with increasing strain, so called yield-point-elongation-like effect (Chen al., 2010). That is because at the beginning stage of deformation, material strength is dominated by dynamic recovery of ferrite due to inhomogeneous strain between duplex structures, which results in a similar yield platform of flow stress curves. At the strain rate of $0.1s^{-1}$, the true strains for yield-point-elongation-like at 900, 950 and 1000 °C are 0.0500, 0.0346 and 0.0264, respectively, decreasing with increasing deformation temperature. The deformation strain stored for dynamic recovery of ferrite at low temperature is larger than that at high temperature, resulting into more obvious dynamic softening.

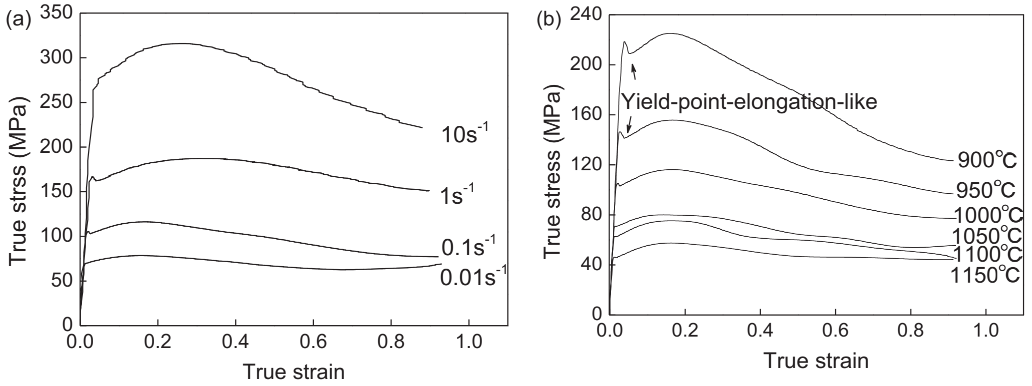

Fig. 1. Flow stress curves obtained at different temperature and strain rate (a) 1050°C, (b) $0.1s^{-1}$.

3.2. Hot deformation equation analysis

The constitutive characteristics of experimental steel was studied, aim at investigating the dynamic recrystallization behaviours and effects of deformation temperature and strain rate on the flow stress by Zener–Hollomon parameter Eq. (1), which reflects how difficult dynamic recrystallization occurs(Han et al., 2011). Eq. (2) is usually used to describe the flow stress evolution with temperature and strain rate as $\alpha\sigma<0.8$, whereas the exponential law (Eq. (3)) is suitable for high flow stress as $\alpha\sigma>1.2$(Xiang et al. 2009). It turns out that hyperbolic sine function (Eq. (4)) gives highest approximation in three kinds of stress function by regression calculation, and the model could be used to analyse the dynamic recrystallization behaviour under any situation.

$$\mathrm{Z} = \dot{\varepsilon}\exp\left(\frac{Q}{RT}\right), \tag{1}$$

$$\dot{\varepsilon} = A_1\sigma^{n_1}\exp\left(-\frac{Q}{RT}\right), \tag{2}$$

$$\dot{\varepsilon} = A_2\exp(\beta\sigma)\exp\left(-\frac{Q}{RT}\right), \tag{3}$$

$$\dot{\varepsilon} = A[\sinh(\alpha\sigma)]^n\exp\left(-\frac{Q}{RT}\right). \tag{4}$$

Fig. 2.a shows the experimental data and regression analysis results of $\ln\dot{\varepsilon}$-$\ln\sigma_p$ plots, indicating the basic linear relationship (Eq. (2)). Whereas the regression results of $\ln\dot{\varepsilon}$ -σ_p plots don't exhibits a closed fitting curves with (Eq. (3)) even at higher temperature and low strain rate, as shown in Fig. 2.b. After taking logarithm for both side of Eq. (4), it can be written as

$$\ln\dot{\varepsilon} = \ln A + n\ln[\sinh(\alpha\sigma)] - \frac{Q}{RT}. \tag{5}$$

Usually the value of α could be calculated from equation of $\alpha = \beta/n_1$ with the value of β and n_1 from the slopes of $\ln\dot{\varepsilon}$ - $\ln\sigma_P$ and $\ln\dot{\varepsilon}$ - σ_P curves, respectively. But due to the slope error of $\ln\dot{\varepsilon}$ - σ_P curves, the value of α was obtained by means of linear programming via 1stOpt15PRO software. Based on Levenberg Marqurdt and global optimization method, the calculated value of Q can be obtained as 294.204 KJ/mol for experimental steel within the range of 900~1150 °C. The value of α, n and A are 0.003470, 3.9284, and 3.167×10^{12}, respectively. Both curves of $\ln\dot{\varepsilon}$-$\ln[\sinh(\alpha\sigma_P)]$and $\ln[\sinh(\alpha\sigma_P)]$-1/T could be seen in Fig. 3, which show better fitting relationships with the hyperbolic sine law. According to calculated value of A, n and Q, peak stress constitution equation of hot deformed experimental steel could be expressed by Eq. (6).

$$Z = \dot{\varepsilon}\exp(\frac{294204}{RT})= 3.167 \times 10^{12}[\sinh(0.00347\sigma)]^{3.9284}. \tag{6}$$

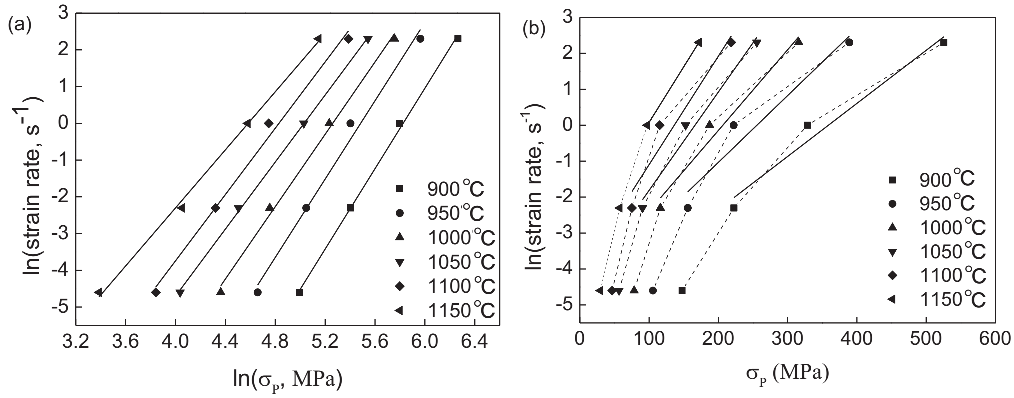

Fig. 2. Relationship between (a) $\ln\dot{\varepsilon}$ and $\ln\sigma_P$; (b) $\ln\dot{\varepsilon}$ and σ_P.

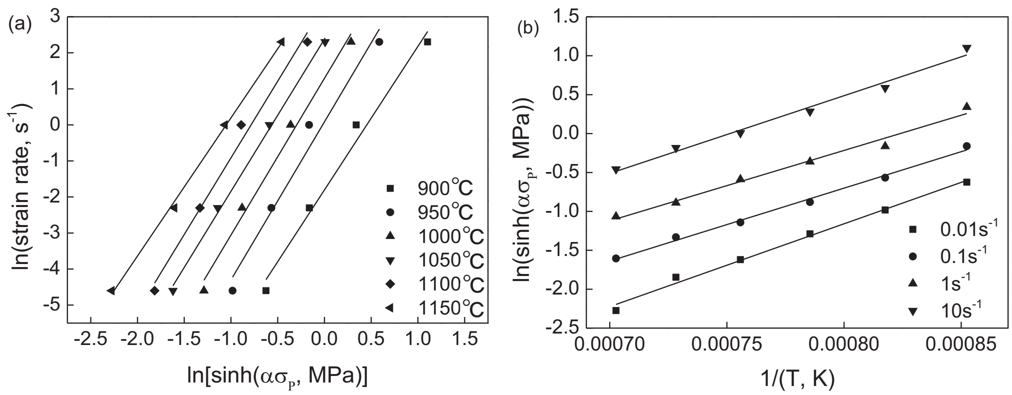

Fig. 3. Relationship between (a) $\ln\dot{\varepsilon}$ and $\ln[\sinh(\alpha\sigma_P)]$; (b) $\ln[\sinh(\alpha\sigma_P)]$ and 1/T.

Activation energy is an important parameter to indicate the difficulty of hot deformation, influenced by the alloy element content (Hamada et al., 2007). The calculated value of Q is far below than that of duplex stainless steel, 460kJ/mol for 2205 duplex stainless steel, for example. The effect of Mn, Al and C elements on activation energy is not high as solute content of Cr, Mo and Ni additions in stainless steels, but quite closed to the calculated Q of 300kJ/mol for 25Mn8Al steel during hot compression (Hamada et al., 2007).

3.3. Structure evolution

It is well known that the flow characteristics of stress-strain curves are determined by microstructure during hot deformation. Fig. 4 shows the duplex structure of experimental at different temperature and strain rate. The central part of hot deformation samples was chosen as the area for microstructure observation, because it represents the real deformation state. With the same temperature of 1050 °C, the recrystallized structure shows a typical dynamic recrystallization evolution of austenite and banded ferrite with increasing strain rate. In Fig .4., corresponding to the deformed microstructure with strain rate of 10 s^{-1}, banded ferrite is distributed in austenite matrix, perpendicular to the compression direction. Tiny austenite structure was obtained by recrystallization and grain size increases with decreasing strain rate. That is because more time is needed for the deformation at low strain rate to get the given strain, and dynamic recovery would decreases intracrystalline defect density and austenite nucleation. At high temperature all or part grain boundary precipitates, which could restrict on grain growth, get dissolved in the matrix. Both reduced nucleation points and grain boundary precipitated would lead to larger austenite size at low strain rate, such as the average recrystallization grain size of ~80 μm for strain rate of 0.01 s^{-1}, as seen in Fig. 4.d. It is evident that the higher strain rate, the smaller austenite grain size.

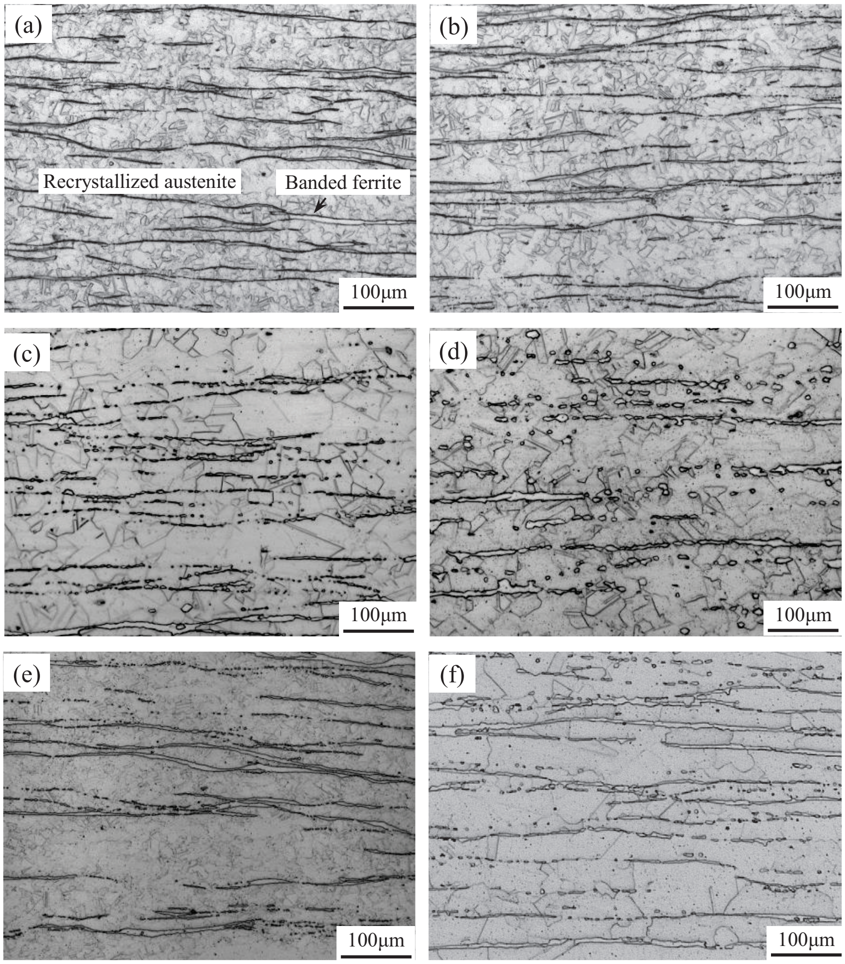

Fig. 4. Optical deformed microstructure with different temperature and strain rate: (a)1050°C, 10s^{-1}; (b) 1050°C, 1s^{-1}; (c) 1050°C, 0.1s^{-1}; (d) 1050°C, 0.01s^{-1}; (e)950°C, 0.1s^{-1}; (f)1150°C, 0.1s^{-1}.

Fig. 4e shows the deformed structure at the temperature of 950 °C and strain rate of 0.1 s^{-1}, it is seen that quantities of fine grain form between banded ferrite, which exhibits characteristics of incompleted recrystallization. As the temperature increased to 1150 °C, coarsened austenite is dispersed in piece ferrite. The calculated transfer temperature from austenite to ferrite is about 1240 °C and there is no phase transformation during the chosen temperature range. But the banded ferrite was distributed in the austenite matrix piece by piece. The interface between dual phases become sharp, and some ferrite seems to be isolated, remaining in austenite matrix. It becomes more obvious with decreasing strain rate and increasing temperature, as seen in Fig. 4f. It could be explained by grain growth for both austenite and ferrite structure. Austenite grain growth dominates at higher strain. Grain boundary expands to outside gradually and separates the banded ferrite into pieces, just like isolated islands. Both higher deformation temperature and lower strain rate could improve ferrite morphology by controlling austenite grain size and avoid formation of cracks during deformation.

4. Conclusions

Characteristics of flow stress for experimental steel during hot deformation were investigated with the conclusions as followed:

(1) The flow stress curves of experimental steel show dynamic recrystallization behaviour with the chosen deformation temperature and strain rate. The peak stress of isothermally compressed steel increases significantly with low temperature and high strain rate. The phenomenon of yield-point-elongation-like effect was observed due to dynamic recovery of ferrite.

(2) Flow stress of experimental curves has a better linear relationship with the hyperbolic sine law. The calculated Q value is 294.204 kJ/mol within the range of 900~1150 °C and Zener–Hollomon parameter could be expressed as $Z = \dot{\varepsilon}\exp(\frac{294204}{RT}) = 3.167 \times 10^{12}[\sinh(0.00347\sigma)]^{3.9284}$.

(3) Dynamic recrystallization behaviour of experimental steel is sensitive to deformation temperature and strain rate, and increasing deformation temperature or decreasing strain rate would promote recrystallization and growth for both austenite and ferrite. And austenite grain growth contributes to evolution of ferrite morphology, from banded structure to pieces.

References

Frommeyer, G., U, B., 2006. Microstructure and mechanical properties of high-strength Fe-Mn-Al-C lihgt-weight TRIPLEX steel. Steel Research Int 9-10, 627-631.

Yoo, J. D., Park, K., 2008. Microband-induced plasticity in a high Mn–Al–C light steel. Materials Science and Engineering: A 496, 417-424.

Suh, D., N.J. Kim, 2013. Low-density steels. Scripta Materialia, 68. 337-338.

Jiménez, J. A., Frommeyer, G., 2010. Analysis of the microstructure evolution during tensile testing at room temperature of high-manganese austenitic steel. Materials Characterization 61, 221-226.

Yang, Y., Yan, B., 2013. The microstructure and flow behavior of 2205 duplex stainless steels during high temperature compression deformation. Materials Science and Engineering: A 579, 194-201.

Balancin, O., Hoffmann, W. A. M., Jonas, J. J., 2000. Influence of microstructure on the flow behavior of duplex stainless steels at high temperatures. Metallurgical and Materials Transactions A 31, 1353-1364.

Momeni, A., Dehghani, K., 2011. Hot working behavior of 2205 austenite–ferrite duplex stainless steel characterized by constitutive equations and processing maps. Materials Science and Engineering: A 528, 1448-1454.

Duprez, L., De Cooman, B. C., Akdut, N., 2002. Flow stress and ductility of duplex stainless steel during high-temperature torsion deformation. Metallurgical and Materials Transactions A 33, 1931-1938.

Wei, H., Liu, G., Xiao, X., Zhang, M., 2013. Dynamic recrystallization behavior of a medium carbon vanadium microalloyed steel. Materials Science and Engineering: A 573, 215-221.

Chen, L., Wang, L.M., Du, X.J., Liu, X., 2010. Hot deformation behavior of 2205 duplex stainless steel. Acta Metallurgica Sinica 35, 52-56.

Han, Y., Zou, D., Chen, Z., Fan, G., Zhang, W., 2011. Investigation on hot deformation behavior of 00Cr23Ni4N duplex stainless steel under medium–high strain rates. Materials Characterization 62, 198-203.

Xiang, J.Y., Song, R.B.,Ren, P.D., 2009. Dynamic recrystallization behavior of 316L stainless steel. Journal of University of Science and Technology Beijing, 31, 1555-1559.

Hamada, A. S., Karjalainen, L. P., Somani, M. C., 2007. The influence of aluminum on hot deformation behavior and tensile properties of high-Mn TWIP steels. Materials Science and Engineering: A 467, 114-124.

Hamada, A. S., Karjalainen, L. P., Somani, M. C., Ramadan, R. M., 2007. Deformation mechanisms in high-al bearing high-Mn TWIP Steels in hot compression and in tension at low temperatures. Materials Science Forum 550, 217-222.